Biomedical Signal Processing and Control 82 (2023) 104566

Contents lists available at ScienceDirect

Biomedical Signal Processing and Control

journal homepage: www.elsevier.com/locate/bspc

Real-time epilepsy seizure detection based on EEG using tunable-Q wavelet transform and convolutional neural network

Mingkan Shen [a,*], Peng Wen [a], Bo Song [a], Yan Li [b]

[a] School of Mechanical and Electrical Engineering, University of Southern Queensland, Toowoomba, QLD 4350, Australia
[b] School of Science, University of Southern Queensland, Toowoomba, QLD 4350, Australia

ARTICLE INFO

Keywords:
CNN
EEG
Real-time
Seizure detection
Tunable-Q wavelet transform

ABSTRACT

Epilepsy is a chronic disease caused by sudden abnormal discharge of brain neurons, leading to transient brain dysfunctions. This paper proposed an EEG based real-time approach to detect epilepsy seizures using tunable-Q wavelet transform and convolutional neural network (CNN). Statistical moments and spectral band power were used to reveal the time domain and frequency domain features in EEG, and then were converted into imaged-like data fed into CNN. The proposed approach was evaluated using the database CHB-MIT. The proposed algorithm achieved 97.57% in accuracy, 98.90% in sensitivity, 2.13% in false positive rate and 10.46-second delay. In addition, the proposed method is suitable in real-time implementation. The outcomes indicate that the proposed method can applied to real-time seizure detection in clinical applications.

1. Introduction

Epilepsy is a chronic non-communicable disease caused by the abnormal synchronous electrical activity of brain neurons [1,2]. It is one of the most common neurological diseases, which affects approximately 50 million people in the world [2,3]. Repeated seizures can cause persistent adverse effects on patients' mental and cognitive functions, and bring life-threatening risks [4]. Therefore, research on the diagnosis and treatment of epilepsy has important clinical significance. Automatic identification of epilepsy seizures from electroencephalogram (EEG) signals and its real-time implementation can provide an objective reference basis for the diagnosis and in time evaluation of epilepsy, thereby reducing the workload of doctors and improving the efficiency of treatment [5]. Bhattacharyya et al. introduced a real-time seizure detection approach through the empirical Wavelet transform method [6]. Disruptive EEG networks for epileptic seizures in real-time application was reported by Bomela et al. [7]. Harmonic Wavelet packet transform with relevance vector machine method was proposed by Vidyaratne et al [2]. Automatic seizure detection based on imaged-EEG signals through fully convolutional networks research was reported by Gómez, C., et al., and they achieved 98.0% in accuracy and 98.3% in specificity result [8]. A deep learning method via two-dimensional deep convolutional autoencoder method was developed by Abdelhameed, A. and M. Bayoumi, and they achieved 98.79% in accuracy and 98.72% in sensitivity [9].

EEG abnormalities in epileptic seizures are mainly manifested as spike waves and sharp waves [10]. Many methods in time, frequency, and time–frequency domains have been developed, such as discrete wavelet transform (DWT), empirical mode decomposition (EMD), Q-wavelet transformation, Hilbert-Huang transform (HHT), mean amplitude spectrum (MAS), tunable-Q wavelet transform (TQWT), etc. [6,11–15]. An important progress in epilepsy seizure detection is the development of machine learning based classification methods. The support vector machine (SVM), linear discriminant analysis (LDA), naive Bayes, logistic regression (LR) and random forest were used to classify the different seizure states in previous studies [11,15–19]. Traditional machine learning methods require manual feature extraction and model matching, while deep learning methods greatly simplify the preprocessing process, which can automatically extract features and complete decoding at the same time. Deep convolutional neural network (CNN) was proposed by Gao et al. and achieved an average classification accuracy of 90% in epilepsy detection [20]. Long short-term memory networks (LSTM) deep learning method was reported by Cao et al., in their experiment, they achieved an 96.3% accuracy [21]. Currently, automatic epilepsy detection can be divided into two types: offline seizure detection and real-time seizure detection. The purpose of offline seizure detection is to identify epileptic seizure signals as accurately as possible from EEG signal [22]. The purpose of real-time seizure

* Corresponding author.
E-mail address: Mingkan.Shen@usq.edu.au (M. Shen).

https://doi.org/10.1016/j.bspc.2022.104566
Received 29 August 2022; Received in revised form 22 November 2022; Accepted 27 December 2022
Available online 4 January 2023

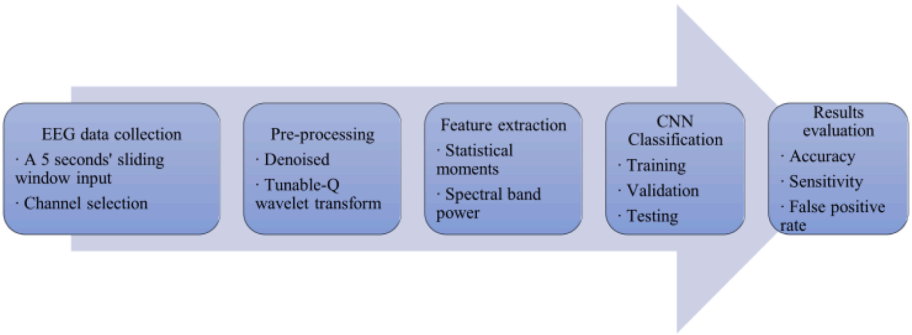

Fig. 1. The framework and main procedures.

Table 1
Data collection from Long-term EEG data Dataset CHB-MIT.

Patient	EEG used (h)	Number of seizures	Seizure duration (s)
Chb01	25	7	40,27,40,51,90,93,101
Chb02	16	3	82,81,9
Chb03	36	7	52,65,69,52,47,64,53
Chb04	25	4	49,111,102,116
Chb05	14	5	115,110,96,120,117
Chb07	28	3	86,96,143
Chb08	16	5	171,190,134,160,264
Chb09	34	4	64,79,71,62
Chb10	20	7	35,70,65,58,76,89,54
Chb17	15	3	90,115,88
Chb18	18	6	50,30,68,55,68,46
Chb19	14	3	78,77,81
Chb20	15	8	29,30,39,38,35,49,35,39
Chb22	15	3	58,74,72
Chb23	14	7	113,20,47,71,62,27,84
Chb24	12	16	25,25,29,25,32,27,19,24,22,19,70,16,27,17,66,68

detection is to identify seizures onsite with the shortest possible delay when the patient has a seizure during continuous EEG monitoring [23].

Samiee et al. used multivariate textural features with gray-level co-occurrence matrix (GLCM) in SVM and reported a 70.19% sensitivity in the real-time seizure detection [24]. As a contrast, time delay embedding method proposed by Zabihi et al. obtained an 89.01% sensitivity [25]. In particularly, graph theory analysis, function connectivity analysis and effective connectivity analysis were used in the seizure detection [15,26–27]. Bomela et al. constructed the network connectivity using Fourier transform to detect the seizure onset and reported 93.6 % sensitivity and a false positive (FP) rate of 0.16 per hour (FP/h) result [7]. A stacked 1D-CNN model is presented via Wang, X., et al. to detect seizure onset automatically and achieved 88.14% accuracy and 0.38% FP rate result [28]. Orthogonal matching pursuit with DWT as pre-processing progress with non-linear features and SVM classifier can also detect the seizure onset in the same dataset. Zarei, A. and B.M. Asl used this method and reported 96.81% sensitivity and 2.74% FP result [29]. Li, C., et al. proposed EMD, common spatial pattern and SVM model get 97.34% sensitivity, 2.5% FP output as well [30]. In our previous work, we achieved 96.15% sensitivity, 96.38% accuracy and 3.24% false positive rate for the real-time seizure onset detection via DWT and RUSBoosted tree Ensemble method [31].

With the recent high-speed development of artificial intelligence techniques in graph classification, research combining signal processing and image classification are used widely in EEG based clinical applications. Chen et al. constructed the imaged-like data via mutual information (MI) brain network matrix based on the EEG attention-deficit/hyperactivity disorder (ADHD) signal as the input of CNN model, and they reported an accuracy of 94.67% on the test data [32]. Ozcan, A.R. and S. Erturk, using 3D-CNN model with an imaged-based approach in seizure prediction work [33]. They converted the statistical moments, Hjorth parameters and spectral band power into 3Dimaged-like data and achieved 85.7% sensitivity and a false prediction rate of 0.096/h in their study. Considering the good performance of this method in other EEG research areas, we applied it in this study by combining the signal processing and image classification in EEG real-time epilepsy seizure detection.

This study aims to develop a seizure detection approach which can be implemented in real-time. In this study, the Butterworth zero-phase filter denoised method and TQWT method were used for the data pre-processing. Statistical moments and spectral band power were calculated to reveal the time domain and frequency domain features to distinguish the seizure-free and seizure active states. The features were then converted into imaged-like data as the input of the CNN models for training and testing using Database CHB-MIT. Finally, the approached is implemented using a 5-second sliding window. All the experiments in this study were carried out in a Dell workstation with dual Intel Xeon E5-2697 V3 CPUs using MATLAB 2021b.

The first section of the paper provides a brief introduction of this study. Section II describes the details of the EEG long-term epilepsy patients' Database CHB-MIT. The pre-processing, feature extraction and CNN model classification are also introduced in this section. Section III reported the work in our experiments and results obtained using the proposed method. Comparisons of previous work using the same datasets were conducted and evaluated in Section IV. Section V concluded the paper.

2. Methodology

In this study, the proposed real-time EEG based seizure detection method includes four major steps using CHB-MIT Database. EEG data from eight channels was selected in this study and the moving sliding window size was selected as 5 s. The Butterworth algorithm was applied to denoise the EEG raw data and TQWT analysis was used to decompose the EEG signal data. After feature extraction, 30 eigenvalues from both time domain and frequency domain features of each EEG channel data were converted into 8*30 imaged-like data as the input of the CNN model to classify seizure free and seizure active subjects for real-time epilepsy seizure detection. The framework of the proposed method is described in Fig. 1.

2.1. EEG data collection

Database CHB-MIT was collected by Boston Children's Hospital with 23 subjects (5 males in age 3–22 years and 17 females in age 1.5–19 years) [34]. The CHB-MIT data was sampled at 256 Hz from 23 bipolar channels by scalp EEG standard 10–20 system caps. In this experiment, 8 electrodes closer to both sides of frontal and temporal regions, such as channel FP1 - F7, F7 - T7, T7 - P7, T7 - FT9, FP2 - F8, F8 - T8, T8 - P8 and FT10 - T8, were used to detect the seizure onset in real-time applications. This study used 16 patients from the CHB-MIT Database, which

Table 2
Extra details of the CHB-MIT Database.

Patient	Gender	Age (y)	Seizure type	Seizure onset zone
Chb01	F	11	SP, CP	Temporal
Chb02	M	11	SP, CP, GTC	Frontal
Chb03	F	14	SP, CP	Temporal
Chb04	M	22	SP, CP, GTC	Temporal, Occipital
Chb05	F	7	CP, GTC	Frontal
Chb07	F	14.5	SP, CP, GTC	Temporal
Chb08	M	3.5	SP, CP, GTC	Temporal
Chb09	F	10	CP, GTC	Frontal
Chb10	M	3	SP, CP, GTC	Temporal
Chb17	F	12	SP, CP, GTC	Temporal
Chb18	F	18	SP, CP	Temporal, Occipital
Chb19	F	19	SP, CP, GTC	Frontal
Chb20	F	6	SP, CP, GTC	Temporal
Chb22	F	9	Not reported	Temporal, Occipital
Chb23	F	6	Not reported	Frontal
Chb24	F	13.5	SP, CP	Temporal

Here, '*GTC*' is generalized tonic-clonic seizures, '*CP*' is complex partial seizures, '*SP*' is simple partial seizures.

excluded patients that had seizures characterized by amplitude depression [14]. The selected subject details are shown in Table 1.

The extra details of CHB-MIT database are summarized in Table 2.

2.2. Pre-processing

In this work, EEG signals were firstly segmented into a 5-second sliding window size with 1-second overlap. A six order Butterworth zero-phase filter between 1 and 50 Hz was used to denoise the raw EEG data. One of the most challenging parts of the EEG based epilepsy seizure detection is to detect the sharp waves and spike waves. However, in different brain rhythms, the features perform differently between different seizure states. TQWT is extensively to decompose an EEG signal into different frequency sub-bands. In TQWT analysis, three adjustable parameters are needed for different signal, which are quality factor 'Q', the redundancy parameter 'r' and the number of levels of decomposition 'j'. The selection of appropriate TQWT parameters significantly affects classification of seizure free and seizure active EEG. The formula of TQWT is shown in formula (1) and (2):

$$G_0^j = \begin{cases} \Pi_{m=0}^{j-1} G_0\left(\frac{\omega}{\alpha^m}\right), |\omega| \leqslant \alpha^j \pi \\ 0, \alpha^j \pi \leqslant |w| \leqslant \pi \end{cases} \tag{1}$$

$$G_1^j = \begin{cases} G_1\left(\frac{\omega}{\alpha^{j-1}}\right) \Pi_{m=0}^{j-2} G_0\left(\frac{\omega}{\alpha^m}\right), (1-\beta)\alpha^{j-1} \leqslant |\omega| \langle \alpha^{j-1} \pi \\ 0, \omega \in [-\pi, \pi] \end{cases} \tag{2}$$

where 'α' is the low-pass scaling of low-pass frequency response '$G_0(\omega)G_0(\omega)$', 'β' is the high pass scaling of high-pass frequency response '$G_1(\omega)G_1(\omega)$' (the conditions $0 < \alpha < 1$, $0 < \beta \leq 1$, and $\alpha + \beta > 1$ is selected to avoid redundancy in signal reconstruction progress), and 'j' is the decomposition level.

The Quality factor 'Q' affects the oscillation behaviour of wavelets and the extent to which the wavelet oscillations are maintained, and expressed as:

$$Q = \frac{2-\beta}{\beta} \tag{3}$$

The redundancy parameter 'r' is the oversampling rate calculated as:

$$r = \frac{\beta}{1-\alpha} \tag{4}$$

In this study, the redundancy parameter 'r' was selected as 3. The redundancy parameter 'r' will be sufficient if $r \geq 3$. For $r \approx 1$, the wavelet will resemble the '*sinc*' wavelet. When $r \geq 3$, the passband of the level-J frequency response will not have a 'flat top' (where the frequency response is equal to a constant over a sub-interval of its passband) [35]. The Quality factor 'Q' was adjusted as 2 and the specified Q-factor should be chosen from $Q \geq 1$. Setting $Q = 1$ leads to a wavelet transform for which the wavelet resembles the second derivative of a Gaussian, and higher values of 'Q' lead to more oscillatory wavelets [35]. In addition, we divided the EEG raw signal into 6 sub-bands when selected $j = 5$, because j levels decomposition corresponds to into $j + 1$ sub-bands [36]. Then, the first 1280 samples of sub-band 2, the first 640 samples of sub-bands 3, 4, 6 and 320 samples of sub-band 5 were selected respectively, which demonstrate significant differences between seizure free and

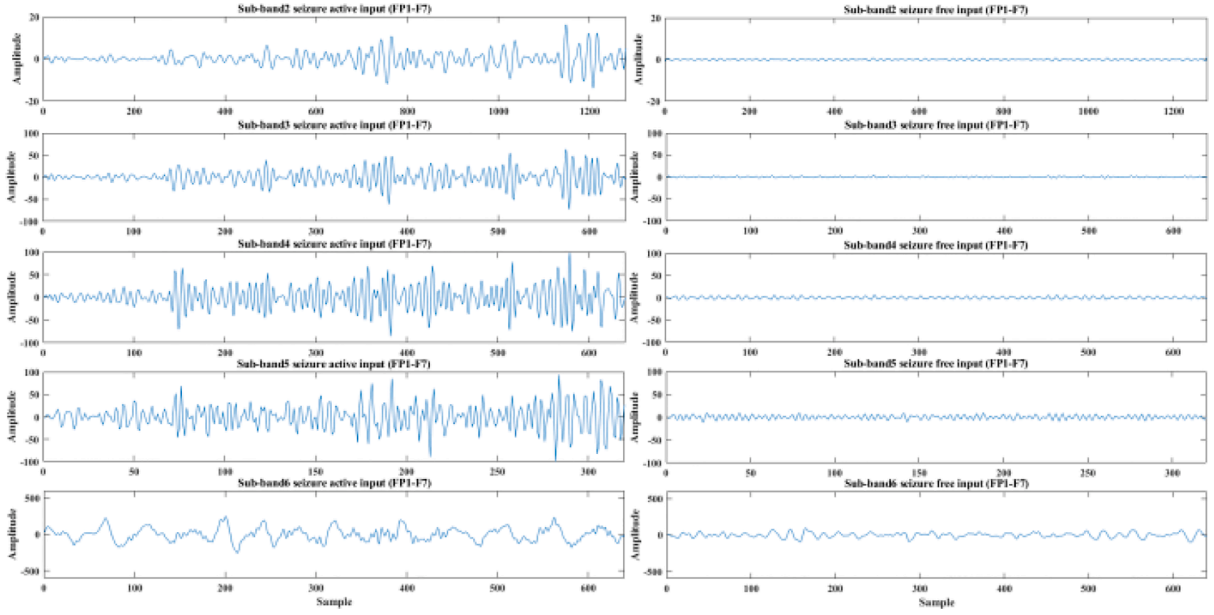

Fig. 2. (a) Sub-band 2 seizure active data, (b) Sub-band 3 seizure active data, (c) Sub-band 4 seizure active data, (d) Sub-band 5 seizure active data, (e) Sub-band 6 seizure active data, (f) Sub-band 2 seizure free data, (g) Sub-band 3 seizure free data, (h) Sub-band 4 seizure free data, (i) Sub-band 5 seizure free data, (j) Sub-band 6 seizure free data. The seizure active input is collected from Chb01_03 from 3006 s to 3011 s data of Channel FP1 – F7, the seizure free input is collected from Chb01_03 from 55 s to 60 s data of Channel FP1 – F7.

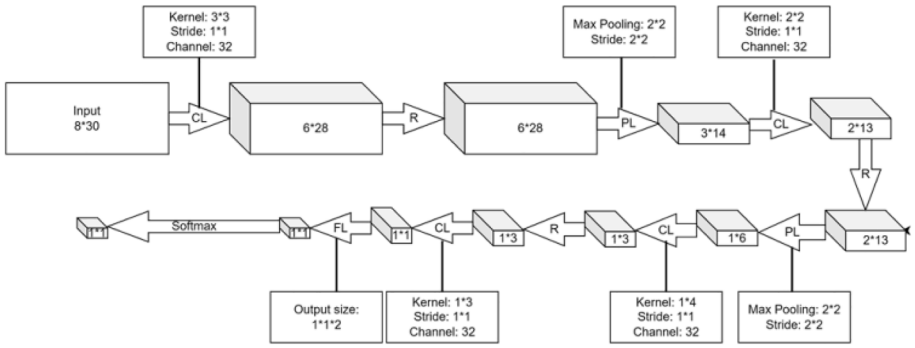

Fig. 3. Diagram of 11-layer CNN architecture, '*CL*' is convolution layer, '*R*' is ReLU, '*PL*' is max pooling layer and '*FL*' is fully connected layer.

Table 3
The architecture of CNN for training and test of the seizure detection.

Layer	Input size	Output size	Trainable parameters
Imaged-data input	8*30*1		
Convolution layer	8*30*1	6*28*32	Kernel size: 3*3 Stride: 1*1 Channel: 32
ReLU	6*28*32	6*28*32	
Max Pooling layer	3*14*32	3*14*32	Pooling size: 2*2 Stride: 2*2
Convolution layer	3*14*32	2*13*32	Kernel size: 2*2 Stride: 1*1 Channel: 32
ReLU	2*13*32	2*13*32	
Max Pooling layer	2*13*32	1*6*32	Pooling size: 2*2 Stride: 1*1
Convolution layer	1*6*32	1*3*32	Kernel size: 1*4 Stride: 1*1 Channel: 32
ReLU	1*3*32	1*3*32	
Convolution layer	1*3*32	1*1*32	Kernel size: 1*3 Stride: 1*1 Channel: 32
Fully Connected layer	1*1*32	1*1*2	
Softmax	1*1*2		

Table 4
The validation accuracy of 16 CNN training models.

Subject for CNN training model	Validation Acc (%)
Chb01	97.38
Chb02	97.29
Chb03	97.50
Chb04	97.51
Chb05	97.43
Chb07	97.20
Chb08	97.10
Chb09	97.10
Chb10	97.06
Chb17	97.63
Chb18	97.65
Chb19	97.27
Chb20	96.91
Chb22	97.27
Chb23	97.08
Chb24	95.74
Mean ± SD	97.20 ± 0.44

'*Acc*' is accuracy.

seizure active states. Detail is shown in the Fig. 2.

2.3. Feature extraction

Five time domain statistical moments from each sub-band were calculated to assess and find the differences in different seizure states. The time domain features contain the standard deviation (SD), mean value, variance, skewness and kurtosis. Furthermore, the frequency domain features were considered in this study as well, we calculated the spectral band power from the denoised EEG data and divided it into five frequency bands, which are δ δ band (1–4 Hz), θ band (4–8 Hz), α band (8–12 Hz), β band (12–30 Hz) and γ band (30–50 Hz) respectively. As a result, 25 time domain eigenvalues and 5 frequency domain eigenvalues were derived for each 5-second sliding window data.

Both SD and variance can be used to describe the degree of dispersion of the signal, and can be obtained as below in formula (5) and (6)

$$SD = \sqrt{\frac{1}{N}\sum_{n=0}^{N}(S_n - \mu)^2} \tag{5}$$

$$Variance = SD^2 = \frac{1}{N}\Sigma_{n=0}^{N}(S_n - \mu)^2 \tag{6}$$

$H(F_i, F_j)$ Kurtosis is a measure of the peak of the probability distribution of a real random variable. High kurtosis means that the increase in variance is caused by extreme differences in low frequencies that are greater than or less than the average. Skewness describes the measure of the asymmetry of a probability distribution function. The formula of kurtosis and skewness is described in formula (7) and formula (8).

$$Kurtosis = \frac{E(x-\mu)^4}{\sigma^4} \tag{7}$$

$$Skewness = \frac{E(x-\mu)^3}{\sigma^3} \tag{8}$$

where 'μ' is the mean value and 'σ' is the SD of the EEG segments, and E(.) is the expectation operator.

In addition, we calculate the percentage of the total power in a specified frequency interval.

$$SpectrualBP(\delta,\theta,\alpha,\beta,\gamma) = \frac{\text{Power}(\delta,\theta,\alpha,\beta,\gamma)}{\text{Power}(1-50\text{Hz})}\% \tag{9}$$

Eight channels were selected in this study, and each channel included 30 eigenvalues. Thus, we construct the imaged-like data into an 8*30 matrix as the input of CNN model.

2.4. Classification via convolutional neural networks

Following the approach based on the VGGNet, a 11-layer CNN was constructed in this study which shown in Fig. 3 [37]. The leaving one out training method and CNN deep learning method were applied to detect seizure onset using Database CHB-MIT.

1) *Leaving one out experiment for Database CHB-MIT*

Sixteen patients' data from Database CHB-MIT (detail shown in Table 1) was used in this part. In leaving one out training method, one subject

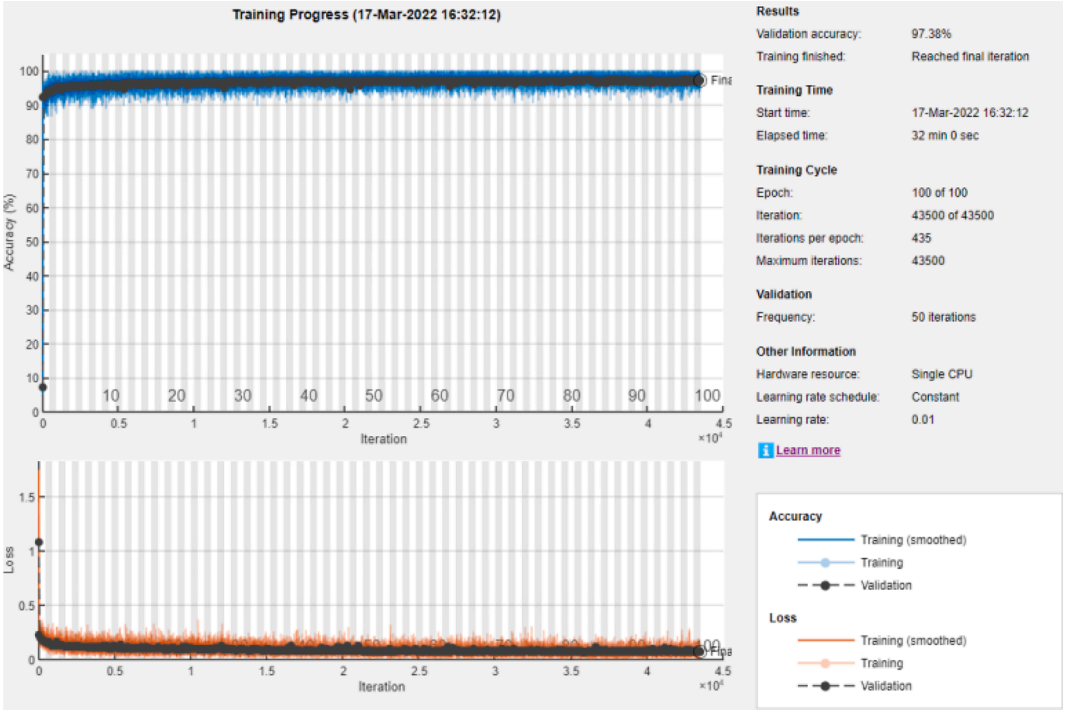

Fig. 4. Training progress for case 'Chb01' based on MATLAB 2021b software.

Fig. 5. Confusion matrix for real-time epilepsy seizure detection for case '*Chb20*'.

data was used for testing, and the other 15 subjects were used for training. As a result, 16 models have been trained.

In this part, the EEG data was segmented into 5-second epoch with a 256 Hz sample rate, which resulted in 1280 sampling points in each epoch. In all 16 subjects, the EEG raw data of 10 min before seizure epochs and 5 min after seizure epochs for each subject data were used to train. The 1-minute interval between the preictal period and the seizure was considered an intervention time and excluded from the training data.

2) *Convolutional neural network*

In this study, the 8*30 size imaged-like data is the input of the CNN model. In CNN model analysis, the training progress selects the learning rate as 0.01, and epochs as 100.

The CNN model includes four convolution layers with batch normalization, two max pooling layers, three ReLU layers and one fully connected layer. The six convolution layers all use 32 filters with convolution kernels of 3*3, 2*2, 1*4, and 1*3, respectively. Batch normalization of each convolution layer is to reduce the internal covariance shift, which can improve training speed and reduce the over-fitting phenomenon. Two Max pooling layers of this architecture are to reduce the cost of training calculation with 2*2 size and 2*2 stride. The activation function ReLU is defined as f(x) = tanh(x) which is used to activate or deactivate a node based on mapped value. The last part is the fully connected layer followed by a Softmax classifier for the identification using the concatenated outputs of the last layers. Table 3

Table 5
Real time detection for Database CHB-MIT using CNN method.

Patient	NS	TP	FP (%)	Sen (%)	Delay (s)	Acc (%)
Chb01	7	7	0.13	100	12.60	99.59
Chb02	3	3	3.74	100	7.36	96.13
Chb03	7	7	0.64	100	6.88	98.97
Chb04	4	4	7.73	100	38.53	91.86
Chb05	5	5	7.96	100	1.03	91.99
Chb07	3	3	4.73	100	3.03	95.22
Chb08	5	5	0.27	100	9.23	98.53
Chb09	4	4	1.50	100	−3.97	98.49
Chb10	7	7	2.71	100	8.32	97.11
Chb17	3	3	0.59	100	15.36	98.98
Chb18	6	5	0.30	83.33	19.43	99.42
Chb19	3	3	0.17	100	10.36	99.65
Chb20	8	8	0.50	100	24.78	99.45
Chb22	3	3	0.58	100	6.03	99.32
Chb23	7	7	1.64	100	−0.97	97.68
Chb24	16	16	0.86	100	9.41	98.70
Total	91	90				
Mean			2.13		10.46	97.57
Sen		98.90				

'*NS*' is the number of seizures, '*TP*' is true positive, '*FP*' is false positive rate, '*Sen*' is sensitivity, and '*Acc*' is accuracy.

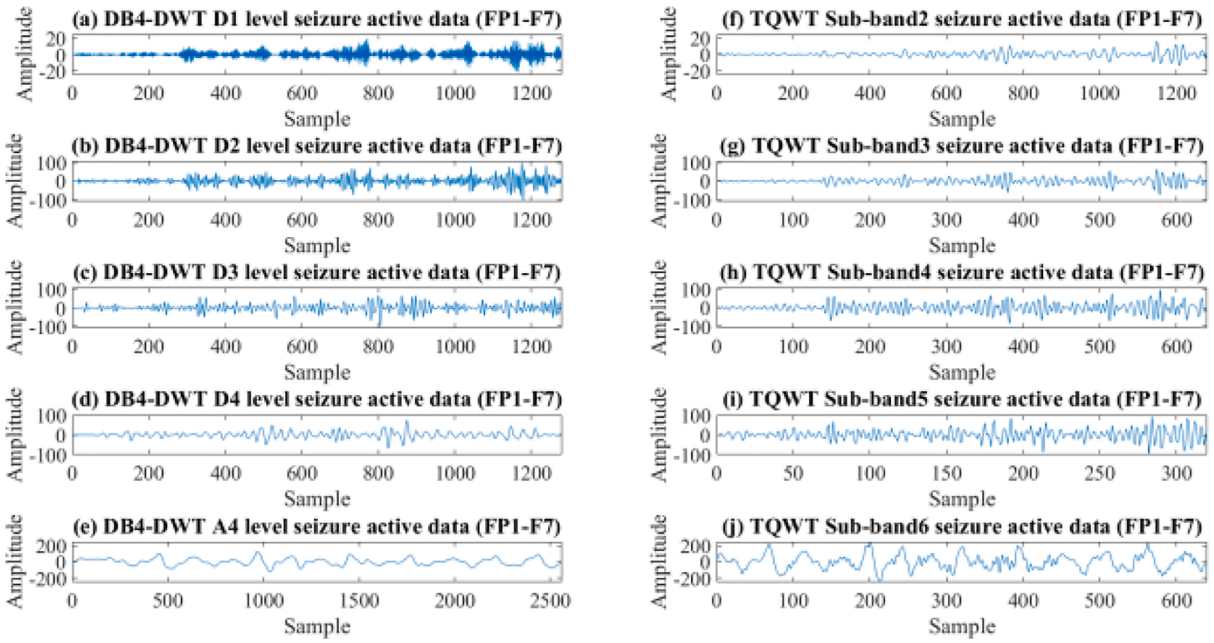

Fig. 6. (a) DB4-DWT D1 level seizure active data, (b) DB4-DWT D2 level seizure active data, (c) DB4-DWT D3 level seizure active data, (d) DB4-DWT D4 level 5 seizure active data, (e) DB4-DWT A4 level seizure active data, (f) TQWT sub-band 2 seizure active data, (g) TQWT sub-band 3 seizure active data, (h) TQWT sub-band 4 seizure active data, (i) TQWT sub-band 5 seizure active data, (j) TQWT sub-band 6 seizure active data. The seizure active input is collected from Chb01_03 from 3006 s to 3011 s data of Channel FP1 – F7.

Table 6
Statistical analysis in TQWT method.

State	Eigenvalue	TQWT decomposition levels				
		Sub-2	Sub-3	Sub-4	Sub-5	Sub-6
Seizure-free	SD	1.3619 ± 2.2613	6.5784 ± 10.3294	10.4072 ± 13.2264	15.0327 ± 17.3020	39.1627 ± 28.2774
	Var	8.0975 ± 64.3944	173.8810 ± 1273.8478	325.4521 ± 1443.8094	609.1218 ± 2319.7164	2790.4187 ± 12547.2178
	Mean	0.0001 ± 0.0015	0.8034 ± 1.5672	−0.0001 ± 0.0069	0.0001 ± 0.0121	−0.0027 ± 0.2678
	SK	0.0011 ± 0.2146	−0.0002 ± 0.0827	−0.0006 ± 0.0870	0.0001 ± 0.0950	0.0936 ± 0.2188
	Kur	6.2395 ± 5.3059	5.3712 ± 4.3218	5.4932 ± 4.4805	5.3152 ± 4.2003	4.7753 ± 2.2624
Seizure-active	SD	3.2849 ± 2.5685	16.3514 ± 12.9003	27.2736 ± 21.5849	40.5403 ± 32.2915	128.3645 ± 82.9969
	Var	19.4455 ± 35.8182	485.7264 ± 893.4722	1357.5774 ± 2472.6776	3016.4642 ± 5510.5715	26905.3477 ± 35389.4594
	Mean	0.0001 ± 0.0032	1.6878 ± 1.2154	−0.0002 ± 0.0149	−0.0003 ± 0.0300	−0.0054 ± 0.7251
	SK	0.0017 ± 0.1900	0.0019 ± 0.0977	−0.0005 ± 0.1015	0.0013 ± 0.1066	0.0635 ± 0.1745
	Kur	7.2427 ± 5.3358	6.5474 ± 4.3414	6.7001 ± 4.6037	6.4038 ± 4.3846	4.1248 ± 1.7769

'Var' is variance, *'SK'* is skewness and *'Kur'* is kurtosis.

Table 7
Statistical analysis in DWT method.

State	Eigenvalue	DWT decomposition levels				
		D1	D2	D3	D4	A4
Seizure-free	SD	2.0692 ± 3.0851	9.2324 ± 12.2004	10.9351 ± 11.5218	9.2463 ± 8.8087	16.5965 ± 11.9710
	Var	15.9233 ± 105.9836	267.2654 ± 1373.9836	294.0855 ± 1184.4718	185.0976 ± 1366.8678	517.8911 ± 2067.3266
	Mean	0.0000 ± 0.0008	1.0804 ± 1.7132	0.0002 ± 0.0068	0.0001 ± 0.0149	0.0003 ± 0.6136
	SK	0.0025 ± 0.0666	0.0044 ± 0.0391	−0.0147 ± 0.0924	0.0194 ± 0.1082	0.0891 ± 0.2362
	Kur	5.7845 ± 5.1579	7.1305 ± 5.7376	6.8999 ± 5.2255	6.1760 ± 2.7626	4.6424 ± 1.7191
Seizure-active	SD	5.2033 ± 4.0940	24.2633 ± 19.1757	32.3770 ± 26.2264	35.4194 ± 31.9827	53.2343 ± 31.8316
	Var	49.0374 ± 89.7095	971.2714 ± 1963.0377	1932.0716 ± 3436.5237	2588.6643 ± 5024.4247	4356.7395 ± 5314.4662
	Mean	0.0001 ± 0.0013	2.4564 ± 1.8062	−0.0001 ± 0.0228	0.0002 ± 0.0635	0.0100 ± 1.4412
	SK	0.0003 ± 0.0724	0.0039 ± 0.0450	0.0022 ± 0.0893	0.0171 ± 0.0901	0.0558 ± 0.1651
	Kur	7.1263 ± 5.1789	8.8929 ± 6.0805	8.0551 ± 5.4553	6.0060 ± 2.8144	3.7751 ± 1.1979

'Var' is variance, *'SK'* is skewness and *'Kur'* is kurtosis.

summarizes the details of the architecture and gives the details of hyperparameter settings in each layer.

In this study, 20% training data is used to validate the CNN model via hold-out validation method and the validation frequency was selected as 50 iterations. In addition, the validation accuracy is listed in Table 4 for 16 CNN models, which shows the performance for each imaged CNN model.

All CNN analysis is implemented using MATLAB 2021b with a single CPU in a Dell workstation of dual Intel Xeon E5-2697 V3 CPUs. The loss and accuracy of training models and validation accuracy were

Table 8
Results of 3 Machine learning methods and proposed methods.

Machine learning methods	Sen (%)	Acc (%)	FP rate (%)
DWT	98.90	96.71	3.02
TQWT	98.90	97.57	2.13

'*Sen*' is sensitivity, and '*Acc*' is accuracy.

summarized in Fig. 4 in the progress of the training data for case 'Chb01′.

The accuracy, sensitivity, FP rate and seizure onset detection delay used to evaluate the proposed method in Database CHB-MIT are defined as below.

Accuracy is a direct parameter in method evaluation, and is defined in formula (10).

$$Acc = \frac{TP + TN}{TP + TN + FP + FN} \tag{10}$$

'*TP*' is the true positive, '*TN*' is the true negative, '*FP*' is the false positive and '*FN*' is the false negative.

Sensitivity is the parameter to measure the ability to recognize the patient cases correctly. In EEG real-time detection, this parameter is used to evaluate the active seizure detection performance.

$$Sen = \frac{TP}{NS} \tag{11}$$

where '*NS*' means the number of seizures.

The seizure onset detection delay represents the difference between the detected seizure onset time and the doctor's marker. Delay is negative if detected the seizure active signal early.

3. Results

3.1. The confusion matrix of real-time seizure detection

The confusion matrix describes all the measures for evaluation in epilepsy seizure detection, which includes the '*TP*', '*TN*', '*FP*', and '*FN*'. The confusion matrix for case '*Chb20*′ detection is shown in Fig. 5.

According to the confusion matrix information, we calculated the accuracy as 99.45% and the false rate as 0.50%. There are 8 seizure active states in this case, and all the seizure active states were detected correctly, so the sensitivity of this case is 100%, and their detection delays were 19.03, 27.03, 33.03, 29.03, 22.03, 19.03, 18.03 and 31.03 s, respectively.

3.2. Real-time seizure onset detection results for Database CHB-MIT

In the real-time application, 240 eigenvalues from 8*30 matrix imaged-like data were selected, and the details of the features selected are shown in Fig. 3 and Fig. 4. CNN model of deep learning method was applied to evaluate the model using leaving one training method. As a result, we received 98.90% sensitivity, 97.57% accuracy, 2.13% FP rate and 10.46 s delay (Table 5).

4. Discussion

4.1. Comparison with other decomposition methods

To compare the performance between TQWT, DB4-DWT and EMD,

Table 9
Results of 3 Machine learning methods and proposed methods.

Machine learning methods	Sen (%)	Acc (%)	FP rate (%)
SVM	76.92	97.83	1.75
KNN	79.12	97.25	2.26
RUSBoosted tree Ensemble	95.60	96.53	3.12
CNN	98.90	97.57	2.13

'*Sen*' is sensitivity, and '*Acc*' is accuracy.

Table 10
Comparison of the proposed method and previous works using CHB-MIT Database.

Reference	Sen (%)	FP (%)	Delay (s)
Bhattacharyya and Pachori (2017) [6]	97.91	0.43	Not reported
Fan and Chou (2018) [40]	97	8.61	6–7
Bomela et al. (2020) [7]	93.6	0.16 per hour	10.06
Wang, X., et al. (2021) [28]	88.14	0.38	Not reported
Li, C., et al. (2021) [30]	97.34	2.5	Not reported
Zarei, A. and B.M. Asl (2021) [29]	96.81	2.74	Not reported
Abdelhameed, A. and M. Bayoumi (2021) [9]	98.72	1.14	Not reported
Our previous work (2022) [31]	96.15	3.24	10.42
Proposed method	98.90	2.13	10.46

'*Sen*' is sensitivity, and '*Acc*' is accuracy.

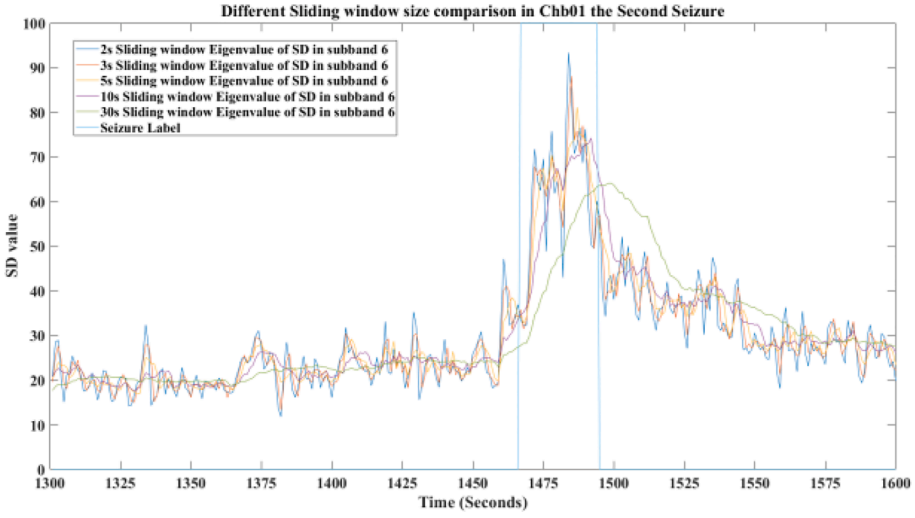

Fig. 7. The eigenvalue SD of the sixth sub-band of TQWT from Channel T7 – P7 in different sliding window sizes for Chb01 second seizure, seizure label line is the seizure active state labelled by doctor from the 1467 s to 1494 s.

the number of decomposition level were all selected as 5. However, the EMD method cannot decompose all 5-sliding window size data into 5 levels. In EMD analysis, parts of seizure-free data can just decompose into 4 levels. Thus, we just compare the performance between TQWT and DWT. In DWT analysis, 5 decomposition levels correspond to 64–128 Hz, 32–64 Hz, 16–32 Hz, 8–16 Hz and 0–8 Hz, respectively. The details of TQWT and DWT were shown in Fig. 6.

To compare performance of TQWT and DWT in this study, the statistical analysis between seizure free and seizure active of training data is conducted. The details of eigenvalues in TQWT and DWT decomposition levels are summarized in Table 6 and Table 7.

The statistical comparison between seizure free and seizure active in this experiment shows that the SD and variance of sub-band 6 in TQWT and A4 level in DWT has most significant difference. Compare with the TQWT and DWT, the difference between seizure free and seizure active in TQWQ of eigenvalue SD and variance is greater but not in eigenvalue mean, skewness and kurtosis. So, we used the CNN model with same architecture to test the performance of the DWT method and the results show in the Table 8.

It is evident that, from Table 8, the TQWT provides a better performance in real-time epilepsy seizure detection which can provide lower FP rate and higher accuracy.

4.2. EEG channel selection and real-time implementation

Channel selection is essential in EEG epilepsy detection, as it can improve accuracy and reduce the computation time. In previous studies, researchers used algorithms, such as the typical spatial pattern, permutation entropy and non-dominated sorting genetic algorithm (NSGA), to select the most significant channels [30,38,39]. After analysing the previous works and the information listed in Table 2 that recorded the details of seizure onset zone in Database CHB-MIT, we found that the electrodes located in the lateral border of the brain have a better performance in epilepsy seizure detections. In this study, we selected eight channels, which are FP1-F7, F7-T7, T7-P7, T7-FT9, FP2-F8, F8-T8, T8-P8 and FT10-T8. Considering the random nature of the epilepsy seizure onset zone for each patient, the aforementioned eight channels were selected to cover the pre-frontal lobe, inferior frontal lobe, temporal lobe and posterior temporal lobe area in both right and left side of the brain.

If the calculation time of each sliding size data is greater than a sliding window overlap (1 s in this study), the real-time implementation would not be possible. The intervention time includes the progress of Butterworth filter denoised, TQWT analysis, eigenvalues calculation and CNN classifier in each 5-second sliding window is 0.03 s. If the sliding window size is too small, the false positive rate will increase. If the size is too large, the results may cause a long-time delay in seizure onset detection due to the increased computational workload. The performance of eigenvalue SD (the sixth sub-band of TQWT from Channel T7 – P7 data) is provided under five sliding window sizes (2 s, 3 s, 5 s, 10 s and 30 s). According to the performance described in Fig. 7, the sliding window is selected as 5 s in this study because of the time delay.

4.3. Performance comparison

We compared three machine learning methods with the proposed CNN model in test data. In the epilepsy seizure detection via TQWT, CNN models, we get 97.57% accuracy, 98.90% sensitivity, and 2.13% FP rate. SVM, KNN and RUSBoosted tree Ensemble methods with random 20% hold-out validation were applied to conduct the EEG epilepsy signal detection and compared with the results of the CNN models. In CNN model, we used 8*30 matrix imaged-like data as input, thus, in these machine learning methods we use the same 240 features as input. The results of these three machine learning methods are summarized in Table 9.

It is obvious in Table 9, the CNN models provide a better performance in real-time EEG epilepsy seizure onset detection than these three machine learning methods. The SVM provides better accuracy and less FP rate, but it just detects 70 of 91 seizures.

Table 10 summarizes the performance of the proposed method and other peer works in the epilepsy seizure onset detection using CHB-MIT Database. The proposed method achieved 97.57% accuracy, 98.90% sensitivity, 2.13% FP rate and 10.46-second delay in real-time seizure onset detection.

5. Conclusion

This study proposed an EEG based real-time epilepsy seizure detection approach using TQWT and CNN models of deep learning method, and evaluated its performance by comparison. In this paper, our proposed method can achieve 97.57% accuracy, 98.90% sensitivity, 2.10% false positive rate and 10.46-second delay in automatic real-time seizure detection implementation in CHB-MIT Database. In addition, we combined signal processing and image classification methods in this experiment. We firstly proposed TQWT method to extract approximate and details of signal and remove redundant information. Furthermore, the comparison also showed that the TQWT is better than DWT in this study which can provide less FP rate. Secondly, we improved the robustness of EEG based epilepsy detection using the deep learning method with CNN model. We also compared the designed CNN model with three machine learning models (SVM, KNN and RUSBoostred tree Ensemble), and find the CNN model can achieve better performance in classifying imaged-like data in this study. At last, the proposed method is suitable for real-time seizure detection in clinical applications as well.

Declaration of Competing Interest

The authors declare that they have no known competing financial interests or personal relationships that could have appeared to influence the work reported in this paper.

Data availability

No data was used for the research described in the article.

References

[1] A.S. Zandi, et al., Automated real-time epileptic seizure detection in scalp EEG recordings using an algorithm based on wavelet packet transform, IEEE Trans. Biomed. Eng. 57 (7) (2010) 1639–1651.
[2] L.S. Vidyaratne, K.M. Iftekharuddin, Real-time epileptic seizure detection using EEG, IEEE Trans. Neural Syst. Rehabil. Eng. 25 (11) (2017) 2146–2156.
[3] R.B. Yaffe, et al., Physiology of functional and effective networks in epilepsy, Clin. Neurophysiol. 126 (2) (2015) 227–236.
[4] D.C. Bergen, Do seizures harm the brain? Epilepsy Curr. 6 (4) (2006) 117–118.
[5] R. Rosch, et al., Network dynamics in the healthy and epileptic developing brain, Network Neurosci. 2 (1) (2018) 41–59.
[6] A. Bhattacharyya, R.B. Pachori, A multivariate approach for patient-specific EEG seizure detection using empirical wavelet transform, IEEE Trans. Biomed. Eng. 64 (9) (2017) 2003–2015.
[7] W. Bomela, et al., Real-time inference and detection of disruptive eeG networks for epileptic seizures, Sci. Rep. 10 (1) (2020) 1–10.
[8] C. Gómez, et al., Automatic seizure detection based on imaged-EEG signals through fully convolutional networks, Sci. Rep. 10 (1) (2020) 1–13.
[9] A. Abdelhameed, M. Bayoumi, A deep learning approach for automatic seizure detection in children with epilepsy, Front. Comput. Neurosci. 15 (2021) 29.
[10] J. Wu, T. Zhou, T. Li, Detecting epileptic seizures in EEG signals with complementary ensemble empirical mode decomposition and extreme gradient boosting, Entropy 22 (2) (2020) 140.
[11] M. Omidvar, A. Zahedi, H. Bakhshi, EEG signal processing for epilepsy seizure detection using 5-level Db4 discrete wavelet transform, GA-based feature selection and ANN/SVM classifiers, J. Ambient Intell. Hum. Comput. (2021) 1–9.
[12] K. Jindal, R. Upadhyay, H.S. Singh, Application of tunable-Q wavelet transform based nonlinear features in epileptic seizure detection, Analog Integr. Circ. Sig. Process 100 (2) (2019) 437–452.
[13] R.J. Oweis, E.W. Abdulhay, Seizure classification in EEG signals utilizing Hilbert-Huang transform, Biomed. Eng. Online 10 (1) (2011) 1–15.

[14] W. Hu, et al., Mean amplitude spectrum based epileptic state classification for seizure prediction using convolutional neural networks, J. Ambient Intell. Hum. Comput. (2019) 1–11.
[15] A. Bhattacharyya, et al., Tunable-Q wavelet transform based multiscale entropy measure for automated classification of epileptic EEG signals, Appl. Sci. 7 (4) (2017) 385.
[16] B. Akbarian, A. Erfanian, A framework for seizure detection using effective connectivity, graph theory, and multi-level modular network, Biomed. Signal Process. Control 59 (2020), 101878.
[17] Y. Gao, et al., Automatic epileptic seizure classification in multichannel EEG time series with linear discriminant analysis, Technol. Health Care (2020(Preprint):) 1–11.
[18] Y.L. Niriayo, et al., Treatment outcome and associated factors among patients with epilepsy, Sci. Rep. 8 (1) (2018) 1–9.
[19] C. Donos, M. Dümpelmann, A. Schulze-Bonhage, Early seizure detection algorithm based on intracranial EEG and random forest classification, Int. J. Neural Syst. 25 (05) (2015) 1550023.
[20] Y. Gao, et al., Deep convolutional neural network-based epileptic electroencephalogram (EEG) signal classification, Front. Neurol. 11 (2020) 375.
[21] X. Cao, et al., Automatic seizure classification based on domain-invariant deep representation of EEG, Front. Neurosci. (2021) 1313.
[22] N. Ahammad, T. Fathima, P. Joseph, Detection of epileptic seizure event and onset using EEG, Biomed Res. Int. (2014. 2014.).
[23] M. Qaraqe, et al., Epileptic seizure onset detection based on EEG and ECG data fusion, Epilepsy Behav. 58 (2016) 48–60.
[24] K. Samiee, et al., Long-term epileptic EEG classification via 2D mapping and textural features, Expert Syst. Appl. 42 (20) (2015) 7175–7185.
[25] M. Zabihi, et al., Analysis of high-dimensional phase space via Poincaré section for patient-specific seizure detection, IEEE Trans. Neural Syst. Rehabil. Eng. 24 (3) (2015) 386–398.
[26] G. Wang, et al., EEG-based detection of epileptic seizures through the use of a directed transfer function method, IEEE Access 6 (2018) 47189–47198.
[27] H. Rajaei, et al., Dynamics and distant effects of frontal/temporal epileptogenic focus using functional connectivity maps, IEEE Trans. Biomed. Eng. 67 (2) (2019) 632–643.
[28] X. Wang, et al., One dimensional convolutional neural networks for seizure onset detection using long-term scalp and intracranial EEG, Neurocomputing 459 (2021) 212–222.
[29] A. Zarei, B.M. Asl, Automatic seizure detection using orthogonal matching pursuit, discrete wavelet transform, and entropy based features of EEG signals, Comput. Biol. Med. 131 (2021), 104250.
[30] C. Li, et al., Seizure onset detection using empirical mode decomposition and common spatial pattern, IEEE Trans. Neural Syst. Rehabil. Eng. 29 (2021) 458–467.
[31] M. Shen, et al., An EEG based real-time epilepsy seizure detection approach using discrete wavelet transform and machine learning methods, Biomed. Signal Process. Control 77 (2022), 103820.
[32] H. Chen, Y. Song, X. Li, A deep learning framework for identifying children with ADHD using an EEG-based brain network, Neurocomputing 356 (2019) 83–96.
[33] A.R. Ozcan, S. Erturk, Seizure prediction in scalp EEG using 3D convolutional neural networks with an image-based approach, IEEE Trans. Neural Syst. Rehabil. Eng. 27 (11) (2019) 2284–2293.
[34] A.L. Goldberger et al., PhysioBank, PhysioToolkit, and PhysioNet: components of a new research resource for complex physiologic signals, Circulation 101 (23) (2000) e215–e220.
[35] I. Bayram, I.W. Selesnick, Frequency-domain design of overcomplete rational-dilation wavelet transforms, IEEE Trans. Signal Process. 57 (8) (2009) 2957–2972.
[36] I.W. Selesnick, Wavelet transform with tunable Q-factor, IEEE Trans. Signal Process. 59 (8) (2011) 3560–3575.
[37] K. Simonyan, A. Zisserman, Very deep convolutional networks for large-scale image recognition. arXiv preprint arXiv:1409.1556, 2014.
[38] J.S. Ra, T. Li, Y. Li, A novel permutation entropy-based EEG channel selection for improving epileptic seizure prediction, Sensors 21 (23) (2021) 7972.
[39] L.A. Moctezuma, M. Molinas, EEG channel-selection method for epileptic-seizure classification based on multi-objective optimization, Front. Neurosci. 14 (2020).
[40] M. Fan, C.-A. Chou, Detecting abnormal pattern of epileptic seizures via temporal synchronization of EEG signals, IEEE Trans. Biomed. Eng. 66 (3) (2018) 601–608.